JOURNAL OF AIRCRAFT
Vol. 46, No. 1, January–February 2009

Identification of Any Aircraft by Its Unique Turbulent Wake Signature

Mark Garnet* and Aaron Altman†
University of Dayton, Dayton, Ohio 45469-0238

DOI: 10.2514/1.38410

The theoretical groundwork for the detection of any aircraft from its unique turbulent wake signature will be discussed, and practical methods to implement this theoretical result will be recommended. During the mid-1990s, NASA conducted research on the detection of atmospheric turbulence using light detection and ranging equipment. This light detection and ranging technology was able to detect turbulent disturbances by the Doppler shift in the frequency of laser-emitted energy that is scattered from atmospheric aerosols. Using this technology, the detection of turbulent disturbances physically created by the passage of aircraft through the atmosphere can be developed. Traditional aircraft detection methods include pulse-Doppler radar systems that measure the frequency shift of radio frequency signals reflected off the skin of an aircraft. This method is currently being defeated by stealth technology. In a military application, light detection and ranging turbulent detection would be able to spot the unconcealable turbulent disturbances caused by aircraft, thereby defeating current stealth technology. In addition, research suggests that turbulent wake generators (i.e., aircraft) have unique turbulent energy signatures. Using the principles of turbulent self-preservation, models can be created to predict both the Reynolds stress and momentum-defect signatures of aircraft as a function of their altitude and airspeed. By using statistical analysis of the turbulent wake, the Reynolds stress or momentum defect can be compared with computed models to determine the identity of the aircraft being targeted. The theoretical and practical manner in which this can be achieved is discussed, and examples of aircraft ranging from the F-15, F-16, F-18, and B-52 are provided.

Introduction

THE modern radar was developed between 1928 and 1940. Although vast advances in radar technology have been made over the last 68 years, the basic operating principals have remained the same. By using the transmission, skin reflection, and reception of RF signals, the position and velocity of moving objects can be measured. Over the last two decades, these basic principals have been defeated by the use of stealth technology. By using multifaceted geometries and radar absorbing materials, air and ground vehicles have been able to reduce their radar cross section, thereby reducing the detection ranges and engagement zones of radar-guided munitions.

During the 1990s, experiments were conducted to detect clear air turbulence (CAT) with light detection and ranging (LIDAR) equipment. Using the transmission and reflection of laser energy off of natural aerosols contained in the atmosphere, turbulent energy and turbulent fluctuations have been detected. The possible applications of this technology are far reaching. Because aircraft produce turbulence from their passage through an atmospheric fluid medium with greater turbulent energy than that produced by CAT, it is only reasonable to assume that the technology exists to detect the turbulent wakes generated by aircraft. As turbulent detection technology matures, its use in military applications becomes extremely appealing in light of the prevalence of methods used to defeat traditional radars.

Military forces must not only detect radar targets but also identify them. Modern air forces typically follow rules of engagement to ensure that friendly aircraft are not inadvertently destroyed during air battles. By using radio communications, computer data links, identification friend or foe systems (IFF), and other technologies, air forces can detect the friendly status of a radar target. These systems can be defeated or simulated with current electronic warfare countermeasures and cannot positively identify the type of aircraft as an enemy. It is reasonable to explore the possibility that aircraft have unique turbulent energies that can be used to identify them as friendly or hostile. Using this theory, a sensor can be used to detect the naturally occurring turbulent wake created by the unknown aircraft and identify its hostile or friendly status.

Received 5 May 2008; revision received 8 August 2008; accepted for publication 8 August 2008.

*Master of Science in Aerospace Engineering; also F-16 Instructor Pilot, Royal Air Force of Oman, Number 18 Squadron, RAFO Thumrait, Post Office Box 732, Postal Code 111, Sultanate of Oman.

†Assistant Professor, Department of Mechanical and Aerospace Engineering, 300 College Park Drive. Associate Fellow AIAA.

Review of the Literature

Turbulence research in the mid-1970s initially concluded that turbulent generators with identical momentum thicknesses resulted in identical turbulent intensities. However, research conducted in 1983 on two-dimensional, turbulent, small-deficit wakes by Wygnanski et al. [1] countered this claim. By taking experimental turbulent intensity and drag calculations on generators tailored to have identical momentum thicknesses, the following conclusions were obtained:

1) Normalized characteristic velocity and length scales depend on the initial conditions.

2) The shape of the normalized mean velocity profile is independent of the initial conditions or the nature of the generator.

3) Normalized distributions of the longitudinal turbulence intensity *are* dependent on the initial conditions.

Additional research performed by George [2] in the late 1980s verified this theory. The implication of this research is that different aircraft with identical momentum thicknesses can produce turbulent intensities that *are* dependent upon the aircraft's geometry. Assuming the existence of appropriate technology, detecting and identifying an aircraft from its unique turbulent intensity signature is feasible. Based on these results, the military requirements of detection and identification of aircraft have, at least in principle, been satisfied.

Detection of Clear Air Turbulence

In 1963, at the 10th Weather Radar Conference for the American Meteorological Society, Smith and Rogers [3] made one of the

earliest suggestions that CAT might be detectable by radar. Previous attempts at detecting CAT had, to various extents, failed using airborne techniques. These techniques included infrared and microwave radiometry, stellar scintillations, laser radar, electric field measurements, air temperature gradients, and vhf radar [4]. Smith and Rodgers made the claim that CAT could be detected by powerful installations that have receivers sensitive enough to detect the weak scattering of radar waves from fluctuations in the refractive index that accompany CAT. Between 1966 and 1970, many ground installations were able to prove Smith and Rodgers correct. However, up until that time, there were no airborne sensors with the ability to detect CAT.

A radio wave propagating through a medium that has a nonuniform refractive index will suffer some loss of energy away from the direction of propagation. The Earth's atmosphere is far from uniform; thus, in addition to refraction, both partial reflection and scattering of radio waves are possible under the appropriate conditions. Since the early 1970s, sensors have been developed to detect the refractivity and reflectivity of an atmospherically turbulent medium [4]. These measured values are instrumental in determining the turbulent dissipation rate of the atmosphere and have been used by meteorologists to quantify turbulent mixing efficiencies.

Radar research has been conducted to detect the turbulence caused by aircraft wakes. In 1980, Noonkester and Richter [5] were able to detect wakes of departing aircraft using radar at a frequency of 3 GHz, at a range of 100–300 m. In 1984, Chadwick et al. [6], using a similar radar, were able to detect the wake turbulence of arriving and departing aircraft using a 200 W radar and a 2.4-m-diam dish at ranges of less than or equal to 1 km. In 1994, Nespor et al. detected vortices of small fighter aircraft in an approach configuration using a 1 MW pulse-Doppler radar with a frequency of 5.6 GHz at ranges of approximately 2.7 km [7]. Gilson, from the Massachusetts Institute of Technology's Lincoln Laboratory, conducted the best-documented and controlled experiment at Kwajalein Atoll in 1992 [8]. The radar cross section of the wake of a C-5A was measured at a range of 15 km using a powerful pulse-Doppler radar with 2–7 MW of peak power.

NASA has also conducted experiments on the detection of aircraft vortices. They have used both radar detection techniques and Doppler LIDAR using infrared frequencies. Although Doppler radar has had some success in the detection of turbulent aircraft wakes, Doppler LIDAR is the more mature of the two detection methods. The underlying principle of pulse-Doppler LIDAR measurements of wind and aerosols is the use of optical heterodyne (coherent) detection, in which laser pulses are transmitted into the atmosphere and scattered off of naturally occurring small dust particles (aerosols) entrained in the ambient flow. From 1997–1998, NASA conducted airborne experiments with the Lockheed L-118C Electra aircraft and with the SR-71 research aircraft. On each airborne platform, a LIDAR sensor was configured to detect CAT in the atmosphere ahead of the aircraft.

Radars and LIDAR equipment can be categorized according to their wavelengths. Doppler radars with wavelengths ranging from 3 to 10 cm can detect the motion of rain, snow, pollens, and insects. They require the presence of a target and cannot detect clear air. Doppler radars with wavelengths of 30 cm to 6 m are called uhf and vhf radars. The radars used to detect CAT belong to this category and can detect the refractive index fluctuations arising from the turbulent mixing of temperature and moisture in the clean air. Pulse-Doppler LIDAR equipment have wavelengths below 10 μm and can detect the motion of aerosol particles. Doppler LIDAR uses the same principle as Doppler radar, but uses shorter wavelengths so that smaller aerosols can be used to trace the wind. Wind speed is relatively small in the atmosphere, and so the corresponding Doppler shift will also be small. With heterodyne detection, there is a mixture of a weak returned signal with a stronger signal close to the returned signal. The difference in the two frequencies is large enough that it can be separated from the original source frequency.

By using Doppler LIDAR to measure the magnitude of horizontal and vertical velocities of turbulence in clear air and the spatial locations of those quantities, the Reynolds stress and mean strain of the flow can be determined. With these values, the turbulent energy production and dissipation of the turbulent flow can be calculated. In addition, LIDAR can measure the streamwise component of a turbulent wake and determine the momentum defect of an aircraft.

Turbulent Self-Preservation

The idea of self-preservation in turbulent flows began during the beginning of the 20th century. Self-preservation is said to occur when the profiles of velocity (or any other quantity) can be brought into congruence by simple scale factors that depend on only one of the variables [2]. There was widespread belief in the turbulence community that flows achieve a self-preserving state by becoming asymptotically independent of their initial conditions. Experiments conducted by Wygnanski et al. [1] were the first to challenge this belief despite widespread acceptance that "turbulence forgets it origins." Experiments conducted by Townsend in 1956 [9] used the velocity scale U_o and the single length scale L_o (which is the half-width of the turbulent wake) to normalize the mean velocity and Reynolds stress. By normalizing in this manner, it was theorized that the mean velocity and Reynolds stress were now independent of the streamwise location. In attempting to verify the results of Townsend's experiments, Wygnanski et al. obtained large differences that could not be attributed to experimental error [1]. Of note were the large variations at large values of $x/(C_D d)$, where C_D was the coefficient of drag, d was the diameter of the turbulent wake generator in the experiment, and x was the streamwise location. Considerations based on the equations of motion show that the momentum thickness, θ, should have been used as the normalizing length scale for the small-deficit wake [1]. This result leads to the conclusion that the total drag force on the generator should have been used to define the initial conditions. The following momentum thickness normalized velocity and length scales were obtained:

$$\left(\frac{U_\infty}{u_o}\right)^2 \approx \left(\frac{x-x_0}{2\theta}\right), \left(\frac{L_o}{\theta}\right)^2 \approx \left(\frac{x-x_o}{2\theta}\right) \tag{1}$$

where $C_D d = 2\theta$.

By using these new normalized length and velocity scales, it was found that different wakes develop differently with downstream distance. During their experiments, Wygnanski et al. [1] constructed multiple turbulent wake generators (cylinders, screens, a solid strip, a flat plate, and a symmetrical airfoil) to obtain the same momentum thickness for each.

As seen in Figs. 1 and 2, the experiments conducted by Wygnanski et al. [1] show that there is a difference in downstream turbulent effects that are resultant from initial conditions. Figure 1 clearly shows that the turbulent intensity distributions (measured at the same downstream location) for three different wake generators produce different results. In Figs. 1 and 2, it is important to note that the horizontal axis, indicated by η, is the nondimensional distance y/L_o.

In 1992, George and Gibson [10] showed that the equations governing homogenous shear flows exhibited self-preservation and

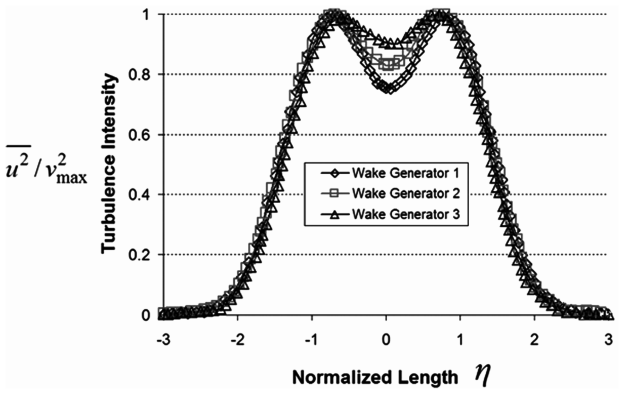

Fig. 1 The normalized turbulent intensity distributions for the three wake generators show that they are distinguishable [1].

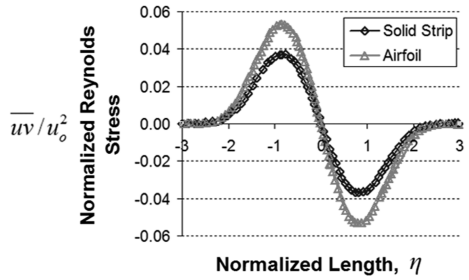

Fig. 2 The distributions of $\overline{uv}/u_o^2$ (nondimensional Reynolds stress) for the solid strip and airfoil show that they are also distinguishable [1].

that these solutions were dependent upon initial conditions. In addition, they found that the ratio of the turbulent energy production rate to its dissipation rate remained constant ($\wp/\varepsilon =$ constant). They also showed that the energy spectra scale over all wave numbers, when normalized with q^2 (Reynolds stress) and λ (Taylor microscale), have shapes determined by initial conditions. $\wp/\varepsilon =$ constant implies that the turbulence Reynolds number (R_ℓ) is constant. George and Gibson discovered that the turbulent energy spectra, when normalized by the Taylor microscale, changed shape based on the type of turbulent generator used. Therefore, every turbulent generator has a unique energy and dissipation spectrum.

Assuming the existence of technology capable of measuring aircraft turbulent production or dissipation spectra, techniques can be developed to identify the aircraft from the measured data.

Turbulent Models

The velocity profile of an object in a turbulent flow can be seen in Fig. 3, in which the velocity profile takes on a Gaussian shape. U_∞ represents the free stream velocity of the flow. The amplitude of the velocity profile (also representing the mean velocity of the velocity profile) is given by the variable U_o. Finally, the wake half-width, defined by the value of $U_o/2$, is given by the variable L_o.

In turbulent flows, velocity fluctuations are created in three dimensions. However, streamwise momentum effects are far greater than the cross-stream momentum effects [11]. As a result, the cross-stream momentum effects can be ignored.

As an aircraft passes through a fluid medium, the viscous interaction of the surface of the object and the surrounding medium causes the fluid to be "carried." This phenomenon can be described using Eq. (2):

$$\rho \int_{-\infty}^{\infty} U(U - U_\infty)\,\mathrm{d}y = M \tag{2}$$

Equation (2) represents the momentum defect per unit volume. If the wake were not present, the momentum defect per unit volume would be ρU_∞. The difference $\rho(U_o - U)$ is the momentum defect (or deficit). The constant M in Eq. (2) is the total momentum removed per unit time from the flow by the obstacle that produces the wake [11].

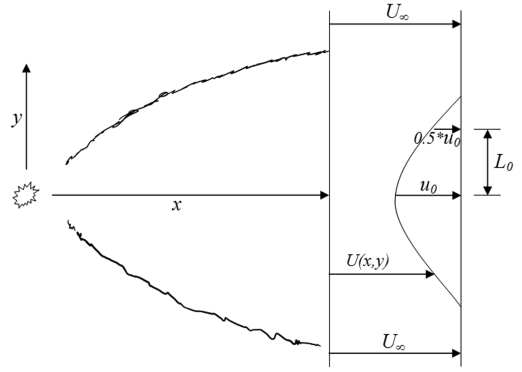

Fig. 3 Sketch defining nomenclature of the momentum wake in turbulent flow 1.

By using Eq. (2), a new length scale can be defined in the turbulent description: momentum thickness. Imagine that a flying aircraft moving through a stationary fluid medium produces a completely separated, stagnant region of width θ. The net momentum defect per unit volume is then ρU_∞, because the wake contains no momentum. The total volume per unit time and depth is $U_\infty\theta$, so that $\rho U_\infty^2\theta$ represents the net momentum defect per unit time and depth. Thus,

$$-\rho U_\infty^2\theta = M \tag{3}$$

The length, θ, is called the momentum thickness of the wake. It can be related to the drag per unit depth of the turbulent generator defined as

$$D \equiv C_{d\frac{1}{2}}\rho U_\infty^2 d \tag{4}$$

Drag is related to momentum where $D = -M$. Through substitution, the definition of drag can be substituted into Eq. (3) to obtain the relation $C_D d = 2\theta$ shown in Eq. (1). As the velocity profile moves downstream, the amplitude (or mean velocity) U_o of the profile decreases, whereas the width, L_o, increases. The magnitudes of both U_o and L_o can be approximated using the relations in Eq. (1).

As stated earlier in this section, the velocity profile in Fig. 3 resembles a Gaussian shape that can be used to describe turbulence statistically. A representative model of the velocity profile of a turbulent generator can be made based off of its coefficient of drag. If the coefficient of drag is known, an estimate of L_o and U_o can be made at a given distance downstream. Those values are used to make a representative velocity profile using a result from Meunier and Spedding [12]:

$$U_1(y) = U_o e^{-y^2/2L_o^2} \tag{5}$$

Because Eq. (5) resembles a Gaussian distribution, it can be said that it is now the probability density function (PDF) of the sample space. With sufficient samples of the turbulent fluctuating velocity to compare with the mean velocity profile model (which is based off of a known coefficient of drag, that is, for an aircraft), the level of probability that the turbulent wake is from that aircraft can be determined. This is because turbulent wakes are self-preserving and depend upon their initial conditions (i.e., aircraft have unique turbulent velocity and energy profiles). Setting a predetermined variance, skewness, and kurtosis can also narrow the identification process of the turbulent wake. If the values of the sample do not fall within those preset limits, then it cannot be said with any degree of accuracy that the turbulent generator is identifiable as a known aircraft.

This discussion represents a nonpropelled body. However, aircraft are considered self-propelled bodies and, thus, have a much different mean velocity profile. As a result, using the momentum-defect technique in this case to provide an accurate analysis would be extremely difficult. The first reason the momentum-defect calculation would be difficult is that a nonaccelerating self-propelled body is in a condition in which thrust equals drag. As a result, the turbulent wake is momentumless. However, the momentum-defect wake can still be seen when the aircraft is decelerating, and a momentum-defect jet is seen when the aircraft is accelerating. Therefore, the momentum defect can only be used to identify aircraft when they are maneuvering. This obviously decreases the amount of time space that is needed for identification. However, the momentum-defect technique would serve well for experimental analysis in a wind tunnel.

In continuing the analysis, other options will now be explored. True momentumless wakes, where $|U_B - U_C| \leq 4\%$, (where U_B is the freestream velocity, and U_C is the velocity of the momentum wake) are extremely difficult to obtain in the laboratory and in nature. A number of conditions can pull the wake far enough away from the momentumless condition and into a completely different regime. The possible perturbations include nonsteady motion of the body, nonsteady motion in the environment, and drag contributions from

waves at boundaries or internally within the fluid. Meunier and Spedding [12] noted that changes in self-propelled bluff body acceleration and deceleration, as well as fluctuations in velocity of the fluid, could cause momentum wakes. These fluid fluctuations are similar to oceanic currents or natural air currents in the atmosphere. Meunier and Spedding derived a relation that determines the mean amplitude of the momentum wake that is corrected for the self-propelled (momentumless) condition. They concluded that if the velocity fluctuations that cause a momentumless wake to exhibit a momentum defect were on the order of 10% of the velocity of the bluff body, the mean absolute amplitude of the momentum wake would be equal to 46% of the amplitude of the wake without self-propulsion. This calculation is not unreasonable. If an aircraft at 6046 m mean sea level (msl) were cruising at 560 km/hr, then approximately 155 m/s of wind is needed (fluid velocity fluctuations) to cause a momentum wake of a nonmaneuvering aircraft. Winds of this velocity occur often at these altitudes. With this in mind, Eq. (5) can be corrected for the self-propelled condition:

$$U_1(y) = 0.54U_o e^{-y^2/2L_o^2} \tag{6}$$

The relations in Eq. (1) are used to find values of L_o and U_o as a function of the momentum thickness and downstream position.

The final and most elegant method of identifying a self-propelled turbulent generator is with the detection of its Reynolds stress. In self-preserved turbulent wakes, the mean profile of the wake diffuses due to the Reynolds stress, which is sustained by the mean shear. The hypothesis of a constant eddy viscosity can be checked for the case of stratified and propelled wakes. If ν_T (eddy viscosity) is constant, then the Reynolds stress profile is proportional to $\tilde{u}_1\tilde{u}_2 = \nu_T(\partial\bar{U}_1/\partial x_2)$. Because the mean profile of the velocity is approximated well by a Gaussian function with amplitude U_o, the Reynolds stress profile should be fit well by the derivative of a Gaussian function with amplitude A and a width L_o' [see Eq. (7)] [12]. An example of a

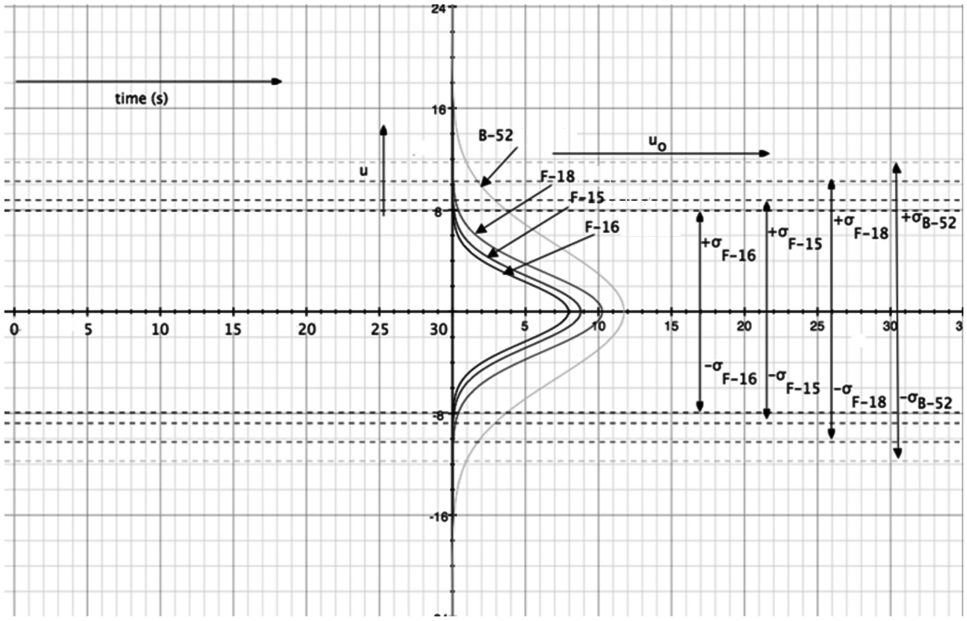

Fig. 4 Self-propelled momentum-defect profiles for the B-52, F-16, F-18, and F-15 and their corresponding standard deviations at $5\Delta x$.

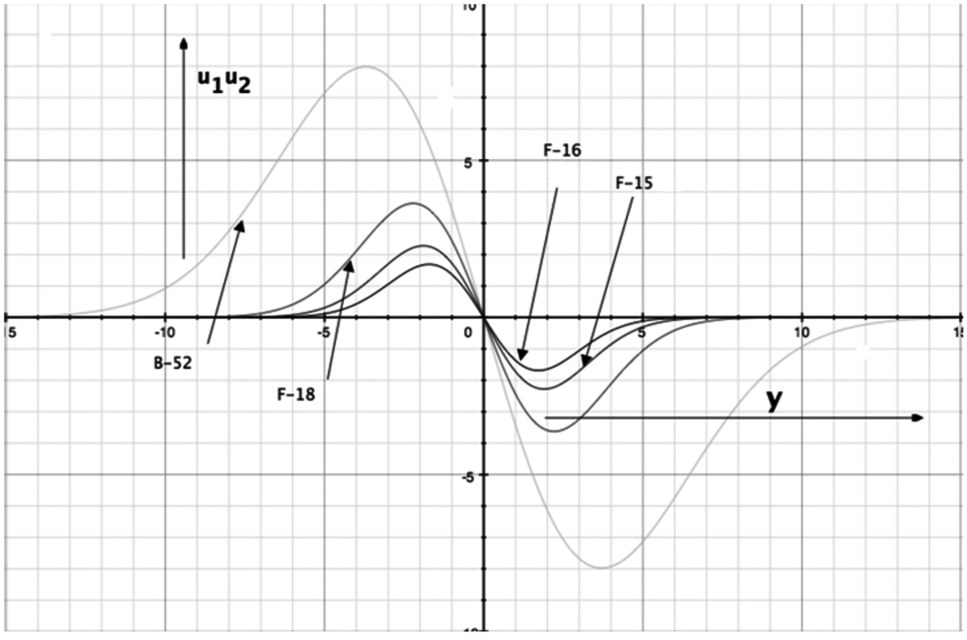

Fig. 5 Reynolds stress profile for the B-52, F-18, F-16, and F-15 at $5\Delta x$.

Table 1 Modeled values for the integral scale, mean rate of strain, Reynolds stress, and turbulent dissipation for the F-16, F-15, and F-18 at $M = 0.85$ and 6064 m, at a distance of $5\Delta x_f$ behind the aircraft

Aircraft type	ℓ, m	$\bar{S}$, s^{-1}	Reynolds stress, m^2/s^2	ε, m^2/s^3
F-16	0.61	24.25	9.56	232
F-15	0.67	24.25	14.3	346
F-18	0.78	24.25	26.5	642

Table 2 Correlation between the measured and modeled values of turbulent energy dissipation (ε) for the F-16, F-15, and F-18

Aircraft type	Measured ε, m^2/s^3	Modeled ε, m^2/s^3	Match, %
F-16	612	232	37.9
F-15	612	346	56.5
F-18	612	642	*95.3*

Reynolds stress profile is shown in Fig. 2.

$$\tilde{u}_1\tilde{u}_2(y) = -A(y/L'_o)e^{-y^2/L'^2_o} \tag{7}$$

The amplitude, A, should be similar to $v_T U_o$, and the width, L'_o, should be similar to the wake width L_o. The value of v_T can be found using the relation $v_T/\nu = c_1 R_\ell$. c_1 is assumed to be on the order of 1.

If the real-time components of velocity can be measured and the Reynolds stress of a self-propelled turbulent generator can be calculated, those values can be compared with the Reynolds stress profile model using Eq. (7). Knowing that R_ℓ is constant (self-preservation) and that A and L'_o are dependent on the momentum thickness of a turbulent generator, the observed Reynolds stress can be compared with a Reynolds stress model created from a known coefficient of drag. If the observed values match the model to a specified degree of accuracy, the identity of the generator could be claimed. In other words, if the Reynolds stress profile of an aircraft in flight can be measured and compared with the Reynolds stress profile models of many known aircraft, a correlation could be made between the observed and model values that are subsequently used to identify the aircraft.

The Detection and Identification of Aircraft

Using the momentum defect and Reynolds stress models presented in Eqs. (6) and (7), a database can be created to determine the unique turbulent signatures of aircraft using known aerodynamic parameters. This database, called the turbulent wake detection database (TWDD), will use known aircraft aerodynamic characteristics. In addition, because turbulent wakes are dependent on downstream distance, aircraft will be placed into categories based upon their primary mission. In this case, aircraft will belong to a fighter, bomber, or transport category. A parametric study was conducted to determine the average length (Δx) of each category. The average length for the fighter category (Δx_f) was determined to be 17.7 m and the bomber category (Δx_b) was 37.7 m. Turbulent calculations in this study were conducted at a downstream distance of $5\Delta x$ with respect to the aircraft's category.

For this study, unclassified data were obtained for the F-15, F-16, F-18, and B-52. An airborne pulse-Doppler or LIDAR sensor would be able to detect clear air turbulence created by these aircraft and use standard radar operating principles to detect their range, altitude, heading, and airspeed. In this example, a radar sensor detects an aircraft traveling at 6046 m msl (20,000 ft.) and Mach = 0.85 (standard atmosphere).

Figures 4 and 5 were created using values from the TWDD and show the modeled momentum defect and Reynolds stress profiles for the F-15, F-16, F-18, and B-52 at 6046 m msl and $M = 0.85$. It is clear even from the figures alone that distinct profiles were created for each aircraft based on both methods.

A pulse-Doppler radar, using a radar range gate sampling of a target's wake at $5\Delta x$ as a function of the selected aircraft category, can take a direct measurement of the turbulent dissipation rate and compare it with the modeled value (Table 1). From the example in Fig. 6, if, in theory, a device was capable of measuring the turbulent dissipation rate of 612 m^2/s^3, then the radar target would most closely correlate to an F-18 (see Table 2). A sensitivity analysis of common atmospheric and minor aircraft turbulent dissipation will be conducted and values at or below those rates will be filtered from analysis. Dissipation rates within $\pm 10\%$ of the modeled value will be considered positively identified. If two or more aircraft models fall within the criteria range, a dual identification, or "mipple," will occur and "enemy" or "friendly" identification will be based on rules of engagement.

Using a pulse-Doppler LIDAR configuration, the sensor could take direct mean velocity measurements of the aerosols within the turbulent flow at a downstream distance of $5\Delta x$. The resulting measurements would then be compared with the momentum-defect models of the aircraft in the TWDD, and a probability of

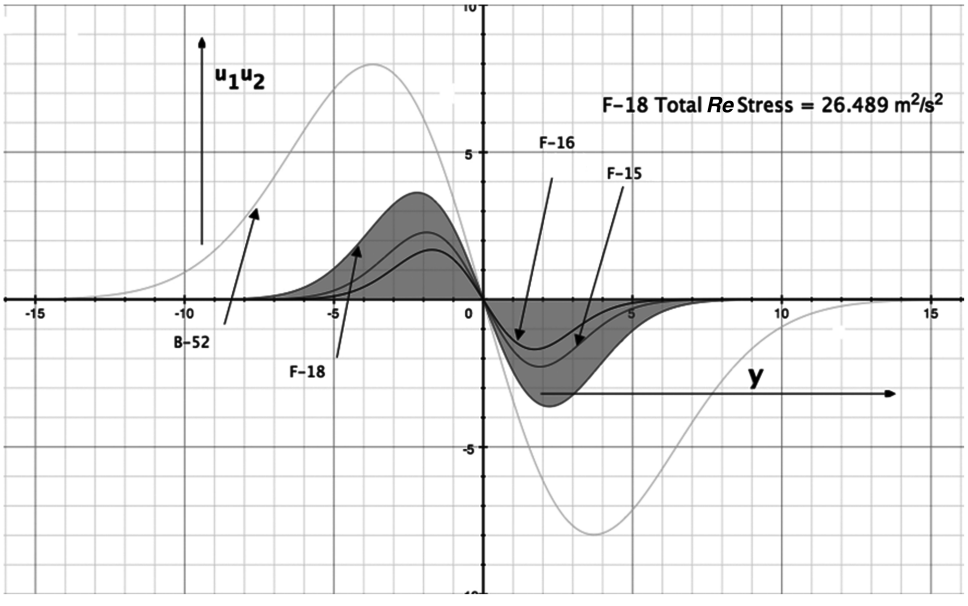

Fig. 6 Total Reynolds stress of the F-18 model shown as the shaded area under the curve.

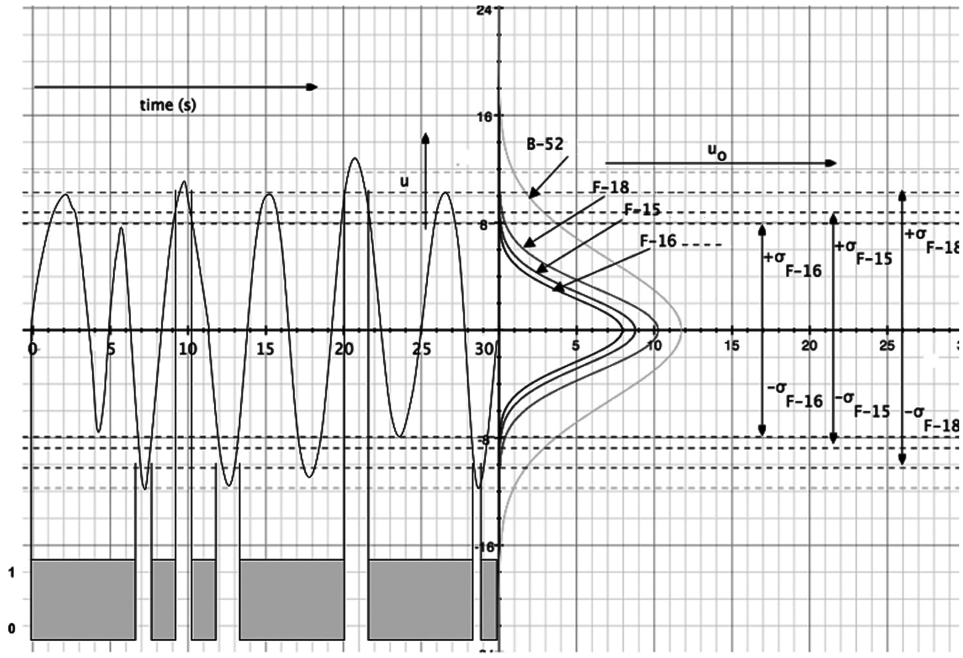

Fig. 7 Instantaneous velocity fluctuations and the correlation to the F-18 PDF.

identification can be obtained by determining the amount of time the fluctuating velocities fell within the respective aircraft's PDF (see Fig. 7 and Table 3). In this example, during the 30 s dwell, an averaged wake velocity of 10.11 m/s and its corresponding velocity fluctuations correlated most closely to the F-18 model.

Conclusions

These results should pave the way for a sensor system that would significantly alter the way aerial warfare is conducted. As emerging nations and their militaries begin to develop low-observable technology, a turbulent detection sensor would be able to detect stealth aircraft by their unconcealable atmospheric disturbances. Additionally, this type of sensor system can *positively* identify the aircraft as an integral part of its operation. This is a significant improvement over current radar systems and dramatically reduces the need to rely on IFF systems. A turbulent sensor system would also be less likely to be defeated by the "Doppler notch" tactic used by fighters to defeat enemy fire-control radars. Finally, due to the fact that the sensor illuminates the far-reaching turbulent wakes of the aircraft and not the aircraft itself, the chances are reduced that enemy onboard radar-warning systems would detect the fact that the aircraft is being targeted. Thus, a turbulent detection sensor can be considered semipassive, relying only on the physical properties of the atmosphere for its operation.

The technology currently exists to create a turbulent detection and identification sensor. Using the well-documented turbulent fundamental principles outlined in this research, a framework has been provided for continued study in this subject area. As a military application, the benefits of detecting stealth aircraft are obvious. However, the ability to *positively* identify aircraft at range solves a major obstacle facing combat pilots today. Through continued support and study, the advent of this type of sensor system will soon become a reality.

References

[1] Wygnanski, I., Champagne, F., and Marasli, B., "On the Large-Scale Structures in Two-Dimensional, Small-Deficit, Turbulent Wakes," *Journal of Fluid Mechanics*, Vol. 168, 1986, pp. 31–71. doi:10.1017/S0022112086000289

[2] George, W. K., "The Self-Preservation of Turbulent Flows and Its Relation to Initial Conditions and Coherent Structures," *Advances in Turbulence*, Hemisphere, New York, 1989, p. 39.

[3] Smith, P. L., and Rogers R. R., *Proceedings of the 10th Weather Radar Conference*, American Meteorological Society, Washington, D.C., 1963, p. 316.

[4] Watkins, C. D, and Browning, K. A., "The Detection of Clear Air Turbulence by Radar," *Physics in Technology*, Vol. 4, No. 1, 1973, pp. 28–61. doi:10.1088/0305-4624/4/1/I01

[5] Noonkester, V. R., and Richter, J. H., "FM-CW Radar Sensing of the Lower Atmosphere," *Radio Science*, Vol. 15, No. 2, 1980, pp. 337–353. doi:10.1029/RS015i002p00337

[6] Chadwick, R. B., Jordan, J., and Detman, T., "Radar Cross Section Measurements of Wingtip Vortices," *Proceedings of Earth Sensor Assembly International Geoscience and Remote Sensing Seminar*, Vol. 1, IEEE Publications, Piscataway, NJ, 1984, pp. 479–483.

[7] Nespor, J., Hudson, E., Stegall, R., and Freedman, J., "Doppler Radar Detection of Vortex Hazard Indicators," CP-10139, Part 2, NASA, Washington, D.C., 1994, pp. 651–688.

[8] Gilson, W. H., "Aircraft Wake RCS Measurement," CR-10139, Part 2, NASA, Washington, D.C., 1994, pp. 603–623.

[9] Townsend, A., *The Structure of Turbulent Shear Flow*, Cambridge Univ. Press, Cambridge, England, U.K., 1956.

[10] George, W. K., and Gibson, M. M., "The Self-Preservation of Homogeneous Shear Flow Turbulence," *Experiments in Fluids*, Vol. 13, No. 4, Aug. 1992, pp. 229–238. doi:10.1007/BF00189015

[11] Tennekes, H. and Lumley, J. L., *A First Course In Turbulence*, MIT Press, Cambridge, MA, 1972, pp. 106–107.

[12] Meunier, P., and Spedding, G., "Stratified Propelled Wakes," *Journal of Fluid Mechanics*, Vol. 552, 2006, pp. 229–256. doi:10.1017/S0022112006008676

Table 3 Correlation of self-propelled momentum-defect average velocity and PDF probability for F-16, F-15, and F-18

Aircraft type	Measured wake avg. velocity, mps	Model wake avg. velocity, mps	Match of model avg. velocity, %	Time within σ of aircraft PDF, s	Total sample time, s	Probability of match, %
F-16	10.11	7.94	78.7	18.1	30	60.3
F-15	10.11	8.78	86.9	18.7	30	62.3
F-18	10.11	10.25	*98.5*	25.8	30	*86.0*